Cellular and Molecular Life Sciences

R432 is a key residue for the multiple functions of Ndt80p in *Candida albicans*

Yun Liang Yang · Chih Wei Wang · Shiang Ning Leaw · Te Pin Chang · I Chin Wang ·
Chia Geun Chen · Jen Chung Fan · Kuo Yun Tseng · Szu Hsuan Huang · Chih Yu Chen ·
Ting Yin Hsiao · Chao Agnes Hsiung · Chiung Tong Chen · Chwan Deng Hsiao · Hsiu Jung Lo

Abstract Ndt80p is an important transcription modulator to various stress-response genes in *Candida albicans*, the most common human fungal pathogen in systemic infections. We found that Ndt80p directly regulated its target genes, such as *YHB1*, via the mid-sporulation element (MSE). Furthermore, the $ndt80^{R432A}$ allele, with a reduced capability to bind MSE, failed to complement the defects caused by null mutations of *NDT80*. Thus, the R432 residue in the Ndt80p DNA-binding domain is involved in all tested functions, including cell separation, drug resistance, nitric oxide inactivation, germ tube formation, hyphal growth, and virulence. Hence, the importance of the R432 residue suggests a novel approach for designing new antifungal drugs by blocking the interaction between Ndt80p and its targets.

Introduction

In the past two decades, the prevalence of invasive nosocomial fungal infections has increased dramatically. *Candida albicans* is the most common human fungal

Y. L. Yang · I. C. Wang
Department of Biological Science and Technology,
National Chiao Tung University, Hsinchu, Taiwan

Y. L. Yang · T. Y. Hsiao
Institute of Molecular Medicine and Bioengineering,
National Chiao Tung University, Hsinchu, Taiwan

C. W. Wang · S. N. Leaw · T. P. Chang ·
J. C. Fan · K. Y. Tseng · S. H. Huang · H. J. Lo (✉)
National Institute of Infectious Diseases and Vaccinology,
National Health Research Institutes, 35 Keyan Road,
Zhunan Town, 350, Miaoli, Taiwan
e-mail: hjlo@nhri.org.tw

C. G. Chen
Institute of Preventive Medicine,
National Defense Medical Center, Taipei, Taiwan

C. Y. Chen · C. A. Hsiung
Division of Biostatistics and Bioinformatics,
Institute of Population Health Sciences, Miaoli, Taiwan

C. T. Chen
Institute of Biotechnology and Pharmaceutical Research,
National Health Research Institutes, Miaoli, Taiwan

C. D. Hsiao
Institute of Molecular Biology, Academia Sinica, Taipei, Taiwan

H. J. Lo
School of Dentistry, China of Medical University,
Taichung, Taiwan

Present Address:
K. Y. Tseng
Institute of Cellular and Systems Medicine,
National Health Research Institutes, Miaoli, Taiwan

pathogen causing systemic infections, especially lethal infections in immunocompromised hosts [1–5]. One of the effective mechanisms for the host innate immune system for defending against microbial pathogens is to produce nitric oxide (NO) [6–8], whereas *C. albicans* responds to NO by rapidly inducing the expression of *YHB1* [9, 10], encoding NO scavengers. Recently, Cta4p was reported to be a positive regulator of *YHB1* [11]. Deletion of *CTA4* prevented *YHB1* transcription during nitrosative stress and increased sensitivity to NO [11].

Candida albicans switches between the unicellular yeast and the filamentous forms to evade unfavorable conditions. The *cph1/cph1 efg1/efg1* double mutant fails to form filaments in vitro and do not cause lethal infections in a mouse model [12, 13]. Tup1p and Nrg1p in *C. albicans* are negative regulators of filamentation [14, 15]. Null mutations on either one lead to hyperfilamention and diminished virulence in vivo [14, 16]. These findings suggest that strains possessing the ability to switch between the yeast and filament forms are those capable of penetrating vital organs and proliferating sufficiently to cause lethal infections.

Ndt80p in *C. albicans* is involved in drug resistance by positively regulating *CDR1* [17]. Great similarity is shared between the C terminus of *C. albicans* Ndt80p and the N-terminus of *Saccharomyces cerevisiae* Ndt80p, a novel DNA-binding domain targeting the mid-sporulation element (MSE, gNCRCAAAA/T) [18]. In contrast, *C. albicans* Ndt80p does not share the same activation domain with *S. cerevisiae* Ndt80p [17, 19], suggesting that these two proteins are associated with distinct functions. Recently, Ndt80p has been reported to regulate different sets of genes in response to different stresses in *C. albicans* [20]. The present study demonstrated that an R432A substitution blocked the functions of Ndt80p in cell separation, drug resistance, NO inactivation, germ tube formation, hyphal growth, and virulence. Hence, the R432 residue in the DNA-binding domain of Ndt80p is important for pathogenesis in *C. albicans* and its vicinity a potential target for drug development. These findings prompted us to employ a virtual screening approach to identifying compounds blocking the interactions between Ndt80p of *C. albicans* and its targets.

Materials and methods

Strains, media, and primers

The *Candida albicans* strains used in the present study are listed in Table 1. Yeast Peptone Dextrose (YPD, 1% yeast extract, 2% peptone, and 2% dextrose), and Synthetic Dextrose (SD, 0.67% yeast nitrogen base without amino acid and 2% dextrose) were prepared as described [21]. Cells were grown in either YPD or SD unless otherwise noted. The compounds for addition to media were from Difco unless otherwise noted. The primers used in the present study are listed in Table 2.

RNA isolation

To avoid filamentous growth, overnight-saturated cultures of the strains were diluted in YP containing 4% glucose [13] pH 6.0 to a starting optical density at 600 nm (OD_{600}) of 0.2 at 37°C. Freshly made $NaNO_2$ (Sigma, SI-S2252) was added to the cultures at a final concentration of 10 mM when the cell density reached OD_{600} of 0.9. The cells were then harvested after additional incubation at 37°C for 30 min. For real-time PCR, total RNA was isolated from the pellets by glass bead beating in the presence of hot acid phenol pH 4.0 (Sigma, P-4682) and RNA lysis buffer (50 mM NaOAc, 10 mM EDTA, 1% SDS). For microarray assay, total RNA was isolated using the mechanical disruption method provided in the RNeasy Midi Kit (Qiagen 75144) according to the recommendation of the manufacturer. An off-column DNase digestion (Baseline-ZERO DNase, Epicentre biotechnologies, Madison, WI, USA) was carried out to ensure complete removal of DNA during the RNA isolation. The RNA quality was measured by Agilent 2100 Bioanalyzer (Agilent Technologies, Santa Clara, CA, USA).

DNA microarray analysis

A total of 25 μg RNAs were directly labeled with Cy3-dUTP or Cy5-dUTP (Perkin-Elmer Life Science, Waltham, MA, USA) using a LabelStar™ Array Kit (Qiagen 28904) according to the manufacturer's instructions. Incorporation of Cy3-dUTP or Cy5-dUTP was performed during the reverse transcription. The labeling efficiencies for the cDNA were measured using a NanoDrop™ 1000 Spectrophotometer (Thermal Scientific, Wilmington, DE, USA) before microarray hybridization. The DNA microarray slides were kindly provided by Dr. S. Rupp at the Fraunhofer Institute for Interfacial Engineering and Biotechnology, Germany. The procedure for prehybridization, hybridization, and wash has been previously described [22]. Finally, the slides were scanned by the GenePix 4000B scanner (Molecular Devices, Sunnyvale, CA, USA). Data were acquired and analyzed by GenePix Pro6.0 (Molecular Devices, Sunnyvale, CA, USA).

Comparison of gene expressions in the presence of $NaNO_2$ in the wild-type (SC5314) versus the *ndt80/ndt80* null mutant (YLO133) consisted of two biological replica. One set of replica was also subjected to a technical duplication with dye-swap. To deal with the systemic dye

Table 1 *Candida albicans* strains used in the present study

Strain	Genotype	Comment	Reference
SC5314		Wild-type	[27]
YLO133	*ura3Δ::λimm434/ura3Δ::λimm434 his1::hisG/his1::hisG arg4::hisG/arg4::hisG ndt80::GFP-Arg4/ndt80::URA3-dpl200 ENO1/eno1::ENO1-tetR-ScHAP4-3xHA-HIS1*	*ndt80/ndt80*	[17]
YLO137	*ura3Δ::λimm434/ura3Δ::λimm434 his1::hisG/his1::hisG arg4::hisG/arg4::hisG ndt80::GFP-Arg4/ndt80::URA3-dpl200::NDT80-HIS1*	*ndt80/ndt80::NDT80*	[17]
YLO263	*ura3Δ::λimm434/ura3Δ::λimm434 his1::hisG/his1::hisG arg4::hisG/ arg4::hisG ndt80::GFP-ARG4/ndt80::URA3-dpl200::ndt80^{R432A}-HIS1*	*ndt80/ndt80::ndt80R^{432A}*	[19]
YLO270	*ura3Δ::λimm434/ ura3Δ::λimm434 his1::hisG/ his1::hisG yhb1::HIS1/yhb1::URA3*	*yhb1Δ/yhb1Δ*	[10]
YLO386	*ndt80Δ-FRT/ ndt80Δ-FRT*	*ndt80/ndt80*	The present study
YLO387	*ndt80Δ-FRT/ ndt80Δ-FRT::NDT80-HA-FRT*	*ndt80/ndt80::NDT80-HA*	The present study
YLO388	*ndt80Δ-FRT/ ndt80Δ-FRT::ndt80^{R432A}-HA-FRT*	*ndt80/ndt80::ndt80^{R432A}-HA*	The present study
YLO464	*ndt80Δ-FRT/ ndt80Δ-FRT::NDT80-FRT*	*ndt80/ndt80::NDT80*	The present study

effect, we adapted quantile normalization, which enforced all distributions of the red and green dye intensities to be as similar as possible. From the normalized intensities, we performed significant analysis [1] to identify the candidate genes in each experiment. The genes with at least twofold difference in expression levels between the wild-type and *ndt80/ndt80* cells are listed in Table 3. For the promoter analysis, it was considered to be a plausible MSE when a sequence matched eight out of the nine nucleotides of MSE.

Quantitative analysis of the mRNA level by real-time PCR

A real-time PCR was performed in a Rotor-Gene^{TM} 3000 instrument (Corbett Research, Mortlake, Australia) with a TITANIUM^{TM} Taq PCR kit (BD Clontech, 639210) and SYBR$^{®}$Green I Nucleic Acid Stain (Cambrex, 50513) to determine the level of mRNA. The sample setup was processed automatically by CAS-1200^{TM} (Corbett Research, Mortlake, Australia). Real-time PCR was performed according to the instructions from the manufacturer and the expressions of *ACT1* and/or *TEF3* in each strain was used as loading controls. The level of mRNA isolated from the wild-type cells in the absence of NaNO$_2$ was defined as one and those from different strains were normalized accordingly.

Assay for cellular sensitivity to nitric oxide

The assay of NO-mediated growth inhibition and concentrations of NO was modified from a previous report [10]. Freshly made NaNO$_2$ (Sigma, SI-S2252) was added to the culture at time zero. Cell growth was monitored after incubation at 37°C for 8 h. Viable cell counts were determined by plate counting on yeast peptone dextrose (YPD) agar medium. The colony-forming unit (CFU) of each strain in the absence of the NaNO$_2$ was defined as 100 and those from the same strain grown in various concentrations of the NaNO$_2$ were normalized accordingly.

Mouse model for virulence

The experiments on the mouse model for virulence were conducted as reported [12]. Briefly, BALB/c mice (white, male) from National Laboratory Animal Center in Taiwan weighing between 18 and 20 g were used to test the virulence of different *Candida* strains. Each *Candida* strain was tested for virulence by injecting 0.5 ml of the cell suspension into the tail vein of the mouse (approximately 1×10^6 cells per mouse). Numbers of mice injected with the wild-type cells, the *ndt8/ndt80* mutant cells, the *ndt80ndt80::NDT80* cells, and the *ndt80/ndt80::ndt80^{R432A}* cells were 17, 17, 9, and 8, respectively. The mice were monitored daily for their survival. These studies were carried out in accordance with the NIH Guide to the Care and Use of Laboratory Animals and the Animal Welfare Act in an AAALAC-accredited program. The animal study protocol for experimental procedures used in the present study was approved by the Institutional Animal Care and Use Committee at the National Health Research Institutes.

Construction of histidine-HA-tagged Ndt80p

Construction of pSFS2A-6H3HA (LOB248): primers HJL1110 containing a sequence of three tandem repeats

Table 2 Primers used in the present study

Name	Sequence	Comment
HJL147	cgg cgg tac cAG GAG ATA TCA TAT CGT T[a]	*NDT80* fragment
HJL148	cgt tct cga gCT GTC TGG ACT TTG TGA	*NDT80* fragment
HJL319	AGA GTT GCC TGA CCA C	Real-time PCR for *NDT80*
HJL320	ATC TGC AAG TCC TCG T	Real-time PCR for *NDT80*
HJL687	ACT AGA GCT TTC GGC A	Real-time PCR for *YHB1*
HJL688	AGG ATC GTA AGG ACC AA	Real-time PCR for *YHB1*
HJL716	ttt tcc gcg gTT GAT GAT GAC GAA GAA AGG	*NDT80* fragment
HJL717	tgt cga gct cGG GTC ATA CTT CAG CAA TG	*NDT80* fragment
HJL 1081	ggtaccTTGTGCCCGAAATAAACCTC	Cloning for full-length *NDT80*
HJL1082	ggg ccc CTG TGG AGG AGT AGG GGT TG	*NDT80* gene
HJL1110	GGA TAC GAC GTA CCA GAT TAC	Histidine-HA-tagged protein
	GCT TAC GAC GTA CCA GAT TAC	
	GCT TAC GAC GTA CCA GAT TAC	
	GCT TAA gag tga aat tct gga aat ctg ga	
HJL1111	GGT ACC GGG CCC CCC CTC GAG	Histidine-HA-tagged protein
	AGA TCT GCC GCA gca tgc GGA TGC	
	CAC CAC CAC CAC CAC CAC GGT	
	GGA TAC GAC GTA CCA GAT TAC GCT	
HJL 1123	ctcgagCCAGTACTTGACGAGTCACT	Cloning for full-length *NDT80*
HJL1174	ACT CCT CCA TCA TTC ATT CAT TCT	CHIP for *YHB1*
HJL1175	TAT GGA AAT CAT GGG GAA GTA AAT	CHIP for *YHB1*
HJL1195	GGG TCA CGT GAT GGT ATT TAA TTT	CHIP for *ADE2*
HJL1196	ATG CGT GTG TGA TGA GAA TAA GAT	CHIP for *ADE2*
HJL1197	CTA ACC CCT CAA TAG CAT TGA TTC	*ADE2* fragment
HJL1197	CTA ACC CCT CAA TAG CAT TGA TTC	*ADE2* fragment
HJL1199	ggt acc gcg gag ctC TAC ATT AGA TGG GGT TGA TT	*ADE2* fragment
HJL1200	GCG ACA CCA CTA GAA AAC TAG	*ADE2* fragment
	AGA TGT GGT GGA TTG GTA TTT	
	CTT TCT GTG	
HJL1201	CAC AGA AAG AAA TAC CAA TCC	*ENO1* fragment
	ACC ACA TCT CTA GTT TCT TAG	
	TGG TGT CGC	
HJL1202	GGT ACC GTG GTG GTG GTG GTG	*ENO1* fragment
	GTG CAT TGT TGT AAT ATT CCT GAA	
	TTA	
HJL1230	ATT AGA ATC AGT TCC ACT CAT GCA	Real-time PCR for *HWP1*
HJL1231	ATA CCA ATA TA GCA GCA CCG AAA	Real-time PCR for *HWP1*
HJL1234	ATC ATT ACC ATC AGG ATC GA	Real-time PCR for *IFG3*
HJL1235	TCA CCC CAA CTT AGA ACA TT	Real-time PCR for *IFG3*
HJL1254	ggg ccc AAT CAA ACT CTT GTC AGA AT	*NDT80* gene
HJL1265	CGG TAA GAG GTC ATC GTC ATA C	Real-time PCR for *RTA2*
HJL1266	TCA GCC AAT TCT GCC ACT C	Real-time PCR for *RTA2*
HJL1271	GGT TAT TGG CTT CAA AGA CA	Real-time PCR for *GIT1*
HJL1272	CTC AAG TAT TGG ACA AAA TCA T	Real-time PCR for *GIT1*
HJL1277	CTT CGT CGA CAA GTT TAT CTT C	Real-time PCR for *CHT3*
HJL1278	CAT CTG GAA TAG TAG CAA CAG T	Real-time PCR for *CHT3*
HJL1301	TCG ATG ATG CCG ATT TGT TA	Real-time PCR for *orf19.1862*
HJL1302	TCG ATG ATG CCG ATT TGT TA	Real-time PCR for *orf19.1862*

Table 2 continued

Name	Sequence	Comment
HJL1303	TTA TCA AGT TGC CGA AAC AT	Real-time PCR for *PST1*
HJL1304	GCA GGG AAA TTA CCA AAT CT	Real-time PCR for *PST1*
HJL1305	TGG TAG TGG ACA TGG CGA TT	Real-time PCR for *ASR1*
HJL1306	TCT TTG TGT GCT TCC TTT TGC	Real-time PCR for *ASR1*
HJL1307	TGA GAA GAA TCA ACG AAG GT	Real-time PCR for *SNZ1*
HJL1308	CAA CAA AAA CAC CAT CAC AT	Real-time PCR for *SNZ1*
HJL1340	GGT TTG GTT ACT TTA GCG TTT C	Real-time PCR for *orf19.308*
HJL1341	TGT GAA TGT GGG TGT GAT ATT T	Real-time PCR for *orf19.308*
HJL1348	TTG CTA ATG CTG GTG TGT TG	Real-time PCR for *FMA1*
HJL1349	TGA CTT TAC CGT TGG TTT TC	Real-time PCR for *FMA1*
HJL1373	CAA AAA ACG TGC TAG ACA TG	Real-time PCR for *RBT4*
HJL1374	GCT TCT TCG TAC CAA GCT T	Real-time PCR for *RBT4*
HJL1375	GAA AAT GAA ACC ATA GCA ACA A	Real-time PCR for *ALS10*
HJL1376	AGC ATT ACC ACC ACC ATT ATT A	Real-time PCR for *ALS10*
HJL1393	ACA CTG ACA GTT ACG GTT CT	Real-time PCR for *DDR48*
HJL1394	CGT ATG AAT CAT CAT TTG AA	Real-time PCR for *DDR48*
HJL1397	TGG CCT GTT TTC TAA AGC CAA GT	CHIP for *FMA1*
HJL1398	CTG CGC TAT ACG GGT TTC C	CHIP for *FMA1*
HJL1409	TCG GAA ATT CTG ACG ATA AAT G	CHIP for *HWP1*
HJL1410	GCG GAT ACA GGT GAT ACA A	CHIP for *HWP1*
HJL1417	AGG CTA TGA TCA ATG GAA AA	Real-time PCR for *SOU1*
HJL1418	TGG CTA AAT GAG TAC ATG CA	Real-time PCR for *SOU1*
HJL1452	TTT CGG CAA CTT TTT CGC	CHIP for *SNZ1*
HJL1453	TCT AAG CCT TTA CAC GTC TC	CHIP for *SNZ1*
HJL1454	AAC CAG AGT GGA GAA TGT	CHIP for *YHB1*
HJL1455	CAA TGT TGG CTT AAT GAA CTT T	CHIP for *YHB1*
HJL1619	gaa ttc TTG GCT CAG CAA CA	*NDT80*-binding domain fragment
HJL1620	ctc gag TTA CTG TGG AGG AGT A	*NDT80*-binding domain fragment

[a] Captial characters present genomic sequence

from hemagglutinin (3× HA, underlined) and HJL977 were used to amplify a 463-base pair (bp) fragment from the pSFS2A vector [23]. The 463-bp fragment was further amplified by primers HJL1111 containing a sequence of six histidines and HJL977 to gain a 529-bp fragment that harbors sequences of two newly introduced restriction sites, *Bgl*II and *Sph*I, as well as six histidines and 3× HAs followed by the *ACT1* terminator. The 529-bp fragment was cloned to the pSFS2A vector to yield pSFS2A-6H3HA (LOB248).

Construction of pSFS2A-*ENO1*p-*NDT80*-6H3HA (LOB 302): The *ADE2* fragment amplified by HJL1197 and HJL1198 was cloned into the LOB248 plasmid to generate LOB298. The DNA fragment from the 3′UTR region of *ADE2* was amplified using primers HJL1199 and HJL1200. The *ENO1* promoter region was amplified using primers HJL1201 and HJL1202. The above two DNA fragments were fused by mixing them together as the template and re-amplification with primers HJL1199 and HJL1202 to generate a 1,348-bp fragment, which was cloned into the LOB298 plasmid to obtain LOB301. The *NDT80* gene was amplified using primers HJL1254 and HJL1082 and then cloned into the LOB301 vector to yield the LOB302 construct containing *NDT80-HA*. Then, the LOB303 was constructed to contain *ndt80*^*R432A*^-*HA*.

Gene disruption of *NDT80* using the *SAT1* flipper cassette was performed according to previously described methods [23]. Briefly, a fragment containing *NDT80* upstream sequences from positions −445 to −322 with respect to the translation start codon was amplified with the primers HJL147 and HJL148, and a fragment containing *NDT80* downstream sequences from positions +1806 to +2120 was amplified with the primers HJL716 and HJL717. The upstream and downstream fragments of *NDT80* were cloned on either side of the *SAT1* flipper cassette in plasmid pSFS2A to result in LOB227. The

Table 3 Genes positively regulated by Ndt80p in *Candida albicans*

Gene name	Potential function	MSE (gNCRCAAAA/T)	Array Wt/*ndt80*	Real-time PCR Wt/*ndt80*
HWP1	Adhesion, filament, morphology	No	17.89	33.2
FMA1	Stress	Yes	8.36	6.2
DDR48	Drug, filament, stress	No	7.18	4.7
RBT4	Drug, morphology, virulence	Yes	5.97	6.5
PST1	Drug, filament	No	4.96	4.0
orf19.251	Drug, stress	Yes	4.96	ND
ALS10	Adhesion, filament, morphology	No	4.91	18.2
orf19.1691	Drug, filament	No	4.26	ND
BUL1	Host (macrophage)	Yes	3.34	ND
orf19.1862	Drug, morphology	No	3.33	2.8
SNZ1	Drug, filament, morphology	Yes	3.19	3.3
orf19.5620	Drug, stress	No	3.16	ND
GIT1	Drug, filament, host (macrophage)	Yes	3.02	3.2
PGA23	Drug	Yes	3.00	ND
FAD3	Drug, stress	No	2.98	ND
MUM2	Filament, morphology, stress	No	2.92	ND
IFG3	Nitric oxide (oxidase), filament	Yes	2.84	2.0
CSP37	Adhesion, virulence	Yes	2.82	ND
HGT20	Glucose transporter	Yes	2.81	ND
CIS2	Filament	Yes	2.80	ND
PRN4	Morphology	No	2.70	ND
YHB1	Drug, morphology, nitric oxide, virulence	Yes	2.59	2.1
FRP6	Host (neutrophils), morphology	Yes	2.58	ND
orf19.4043	Stress	Yes	2.56	ND
DUT1	Stress	No	2.52	ND
orf19.4216	Drug, filament, morphology	Yes	2.51	ND
orf19.6840	Drug	Yes	2.48	ND
orf19.1724	Nitric oxide	No	2.46	ND
orf19.1152	Morphology, stress	Yes	2.45	ND
NIP1	Host (macrophage)	No	2.38	ND
RTA2	Drug, stress	No	2.37	2.8
orf19.4690	Nitric oxide	Yes	2.37	ND
CHT3	Filament, stress	No	2.31	2.4
orf19.2125	Morphology	No	2.26	ND
orf19.308	Morphology	Yes	2.25	1.8
orf19.7350	Drug, stress	No	2.23	ND
orf19.2496	Drug	Yes	2.20	ND
ASR1	Drug, morphology, stress	No	2.14	1.8
SOU1	Drug, filament, morphology	Yes	2.12	2.6
PLB4.5	Morphology	Yes	2.11	ND

Wt wild-type SC5314 strain, *ndt80 ndt80/ndt80* null mutant strain, *ND* not determined

codon region of *NDT80* was replaced by the *SAT1* flipper through a double cross-over to generate the YLO386 strain. To tag Ndt80p with histidine-HA via the genomic locus, we applied *Sac*I restriction digestion to LOB302 and LOB303 plasmids and then introduced the resultant DNAs into YLO386 separately to generate YLO387 (*ndt80/ndt80::NDT80-HA*) and YLO388 (*ndt80/ndt80::ndt80*^R432A^-*HA*), respectively. The DNA fragment containing a full-length

NDT80 along with its promoter region was amplified by primers HJL1081 and HJL1123. The DNA fragment was cloned into pGEMT-easy vector and then sub-cloned into LOB227 by *Kpn*I and *Xho*I digestion to result in the LOB387. We applied *Kpn*I and *Sac*I restriction digestion to LOB387 plasmid and then introduced the resultant DNAs into YLO386 to generate YLO464 (*ndt80/ndt80::NDT80*).

Chromatin immunoprecipitation

The *C. albicans* cells were treated with freshly prepared 10 mM $NaNO_2$ at 37°C for 30 min before being harvested. Cells were cross-linked with 1% formaldehyde (Merck, 1.04003.100) and then lysed in lysis buffer (50 mM HEPES, pH 7.5, 500 mM NaCl, 1 mM EDTA, pH 8.0, 0.1% Triton X-100, 0.1% sodium dodecyl sulfate, 0.1% sodium deoxycholate) supplemented with a protease inhibitor cocktail (ROCHE, 04 693 132 001), using the FastPrep-24 instrument (MP Biomedicals, Illkirch, France) at a speed of 6 m/s for 40 s, four times with cooling intervals. The chromatin was sheared to an average size of 500 bp by a Bioruptor (Diagenode, Liege, Belgium). Portions of the input sample (50 μl) was retained as the genomic DNA control and the remaining (500 μl) was incubated with 2 μg of HA antibody (Abcam, ab9110), rotated at 4°C overnight, and subsequently incubated with 100 μl of protein A agarose (Upstate, 16–156) at 4°C for 4 h. Agarose beads were then washed and the DNA was eluted by TES buffer (50 mM Tris-HCl, pH 8.0, 10 mM EDTA, 0.1% SDS). Cross-linking was reversed by incubating the DNA solution at 65°C overnight. Finally, proteins were removed by the phenol/chloroform/isoamyl alcohol method and DNA precipitation was facilitated by adding 20 μg of glycogen (Invitrogen, 10814-010). To normalize the PCR efficiency for different primers, the amount of promoter DNA amplified from 25 ng of genomic DNA was defined as one and those from the CHIP resultants were normalized accordingly. Ndt80p should not associate with the *ADE2* promoter in vivo. Therefore, the value of the *ADE2* DNA fragments in each immunoprecipitation was the result of non-specific background and was used for secondary normalization to determine the ratio of change for particular promoters from the same strain.

Electrophoretic mobility shift assays

Nuclear protein was extracted as described previously [24]. Briefly, spheroplasts were prepared by incubating cells in 20 ml of YPD with 1.1 M sorbitol containing 400 U/ml lyticase (Sigma, L4025) for 30 min. Crude nuclei were extracted by douncing the spheroplast in breaking buffer (18% Ficoll, 1% thiodiglycol, 5 mM Tris-HCl, pH 7.4,

20 mM KCl, 2 mM EDTA-KOH, pH 7.4, 0.125 mM spermidine, 0.05 mM spermine) for 20 times and subsequently centrifuging at $5,000 \times g$ twice for 12 min each at 4°C to remove non-spheroplasting cells. Finally, crude nuclei were harvested by centrifugation at $24,000 \times g$ for 15 min at 4°C followed by suspension in ice-cold buffer B (100 mM Tris-acetate, pH 7.9, 50 mM potassium acetate, 10 mM $MgSO_4$, 20% glycerol, 2 mM EDTA-KOH, 3 mM DTT, $1\times$ protease inhibitor cocktail), while adding $(NH_4)_2SO_4$ to a final concentration of 0.9 M before being stirred for 30 min at 4°C. The samples were then centrifuged at $215,000 \times g$ for 30 min. The supernatant was recovered and desired amount of $(NH_4)_2SO_4$ was added to attain 75% saturation. The pellet containing nuclear proteins were harvested, dissolved, and dialyzed in buffer C (20 mM HEPES, pH 7.6, 10 mM $MgSO_4$, 10 mM EGTA, 20% glycerol, 5 mM DTT, 0.5 mM PMSF).

Gel shift assay was performed by the electrophoretic mobility shift assay "Gel Shift" Kit (Panomics, Fremont, CA, USA) according to the manual. Briefly, 4 μg of total nuclear proteins or 0.3 μg of purified N, C-terminally tagged $Ndt80_{221-529}$-hexa-His from *E. coli* along with 1 μg Poly d(I-C) was incubated in $1\times$ binding buffer at room temperature for 5 min. The sample was then combined with the biotin-labeled double-stranded MSE probe (200 fmol) and incubated at 15°C for 30 min. DNA-protein complexes were then resolved by electrophoresis on a 6% native polyacrylamide gel and transferred to the membrane (GeneScreen Plus® Hybridization Transfer Membrane, Perkin-Elmer, NEF988001PK). A DNA fragment containing the putative *YHB1* MSE (GAA TAT TAC ACA AAA CCG CGG AA) was used as the probe. The shifted bands were detected by the HRP-conjugated Streptavidin. The unlabelled MSE probe or a single base substituted mutant probe (GAA TAT TAC AgA AAA CCG CGG AA) was used to perform competition analyses.

Construction and purification of Ndt80p in *Escherichia coli*

The N, C-terminally tagged $Ndt80_{221-529}$-hexa-His plasmids were constructed by cloning a PCR-generated fragment containing the Ndt80p DNA-binding domain, using HJL1619 and HJL1620 primers, into the *Eco*RI and *Xho*I sites of pET42a (Novagen). Protein was expressed in C43 *E. coli* cells (Novagen), and positive clones were checked by PCR, restriction analysis and Western-blot analysis using anti-hexa-His antibodies (Sigma). Protein expression was induced by the addition of IPTG. Crude extracts were filtered through 0.45 μm and passed over a Ni-NTA column (GE Healthcare). The protein was eluted with an imidazole gradient ranging from 50 to 400 mM.
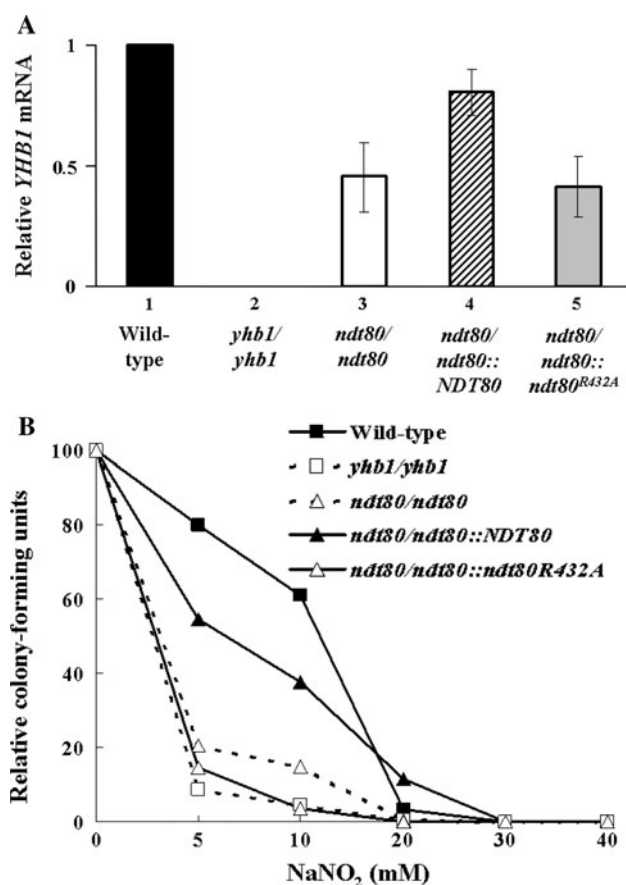
Fig. 1 The level of *YHB1* mRNA and nitric oxide inactivation. **A** Real-time PCR was applied to measure the mRNA level. Values on the *vertical axis* represent the relative mRNA expression level of *YHB1* genes in various strains grown in the presence of 10 mM NaNO₂. *Bar 1* wild-type cells (SC5314); *bar 2 yhb1/yhb1* mutant cells (YLO270); *bar 3 ndt80/ndt80* mutant cells (YLO133); *bar 4 ndt80/ndt80::NDT80* cells (YLO137), and *bar 5 ndt80/ndt80::ndt80^{R432A}* cells (YLO263). **B** NO sensitivity assay. Values on the *horizontal axis* represent the concentrations of NaNO₂ and those on the *vertical axis* represent relative colony-forming units per ml

Further purification was carried out with GSTrap (GE Healthcare) with PBS pH 8.0 containing 10 mM glutathione. The proteins in the collected fractions were concentrated with Centricons (Millipore), dialyzed against PBS, and digested by thrombin before further purification by gel-filtration (Superdex 200) chromatography. The resulting protein was concentrated to 6.8 mg/ml in a buffer containing 10 mM Tris pH 7.8, 100 mM NaCl, and 1 mM DTT.

Results

Target genes of Ndt80p

A total of 40 potential targets of Ndt80p (Table 3) were identified by expression profiling based on DNA microarray analyses. The promoters of 22 of them contained a plausible MSE site. These 40 genes have one or multiple potential functions. There were three genes involved in adhesion, three in virulence, four in host interaction, 13 in filamentous growth, 16 in morphology, and 27 in stress responses (including drug and nitric oxide) response. The expressions of 16 of those 40 potential targets were verified by real-time PCR (Table 3).

Ndt80p is involved in nitric oxide inactivation

In the present study, we found that null mutations in *NDT80* reduced the expression of *YHB1* (Fig. 1A, bar 1 vs. bar 3), which is consistent with the previous report [20]. Nevertheless, this expression was not completely abolished in the *ndt80/ndt80* mutant cells because Ndt80p is not the sole positive regulator of *YHB1*. As expected, the level of *YHB1* expression was restored in the mutants by introducing a wild-type *NDT80* allele (Fig. 1A, bar 3 vs. bar 4).

We then sought to investigate the biological effect of the mutated Ndt80p on the NO sensitivity. The *ndt80/ndt80* null mutant was more sensitive to NaNO₂ than the wild-type was, a behavior shared with the *yhb1/yhb1* mutant (Fig. 1B). A wild-type *NDT80* allele restored the growth of the *ndt80/ndt80* null mutant (Fig. 1B, *ndt80/ndt80::NDT80*), indicating that the increased sensitivity was indeed due to the *NDT80* knockout. All strains were killed when the concentrations of the NaNO₂ were higher than 30 mM (Fig. 1B). Interestingly, after NaNO₂ treatment, the *ndt80/ndt80* mutant cells form as few colonies as *yhb1/yhb1* mutant cells did even though the expression of *YHB1* in the *ndt80/ndt80* mutant cells was approximately half of that in the wild-type cells. The observation that *yhb1/YHB1* heterozygous mutant cells have similar NO sensitivity as the wild-type cells [10] rules out the possibility that the sensitivity to NO in *ndt80/ndt80* mutant cells solely resulted from 50% reduction of *YHB1* expression. Hence, down-regulations of other Ndt80p target genes involved in NO inactivation, such as *IFG3*, orf19.1724, and orf19.4690, may also contribute to the sensitivity to NO in *ndt80/ndt80* mutant cells.

Ndt80p is important for cell separation, germ tube formation, and hyphal growth

Here we further determined whether Ndt80p was also involved in other functions. The *ndt80/ndt80* mutant cells were defective in cell separation (Fig. 2Ab). Furthermore, the wild-type cells formed germ tubes in liquid media containing serum (Fig. 2Ba). In contrast, the *ndt80/ndt80* mutant cells formed a chain of cells similar to pseudohyphae and failed to form germ tubes in the presence of serum (Fig. 2Bb). As expected, the *ndt80/ndt80* mutant

Fig. 2 Assays for cell separation, germ tube formation, and hyphal growth. Four strains, including (*a*) wild-type (SC5314), (*b*) *ndt80/ndt80* (YLO386), and (*c*) *ndt80/ndt80::NDT80* (YLO464), and (*d*) *ndt80/ndt80::ndt80* ^{R432A} (YLO388) were studied. **A** Cell separation. Cells were grown on agar YPD medium at 30°C overnight. **B** Germ tube formations. Cells were grown in liquid YPD medium containing 10% fetal bovine serum at 37°C for 3 h. **C** Hyphal growth. Cells were grown on agar medium containing 4% fetal bovine serum at 37°C for 4 days. The *scale bar* is 50 μm
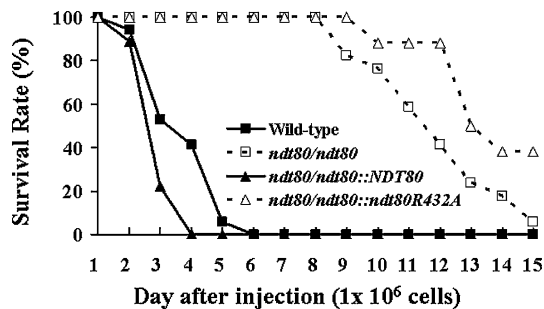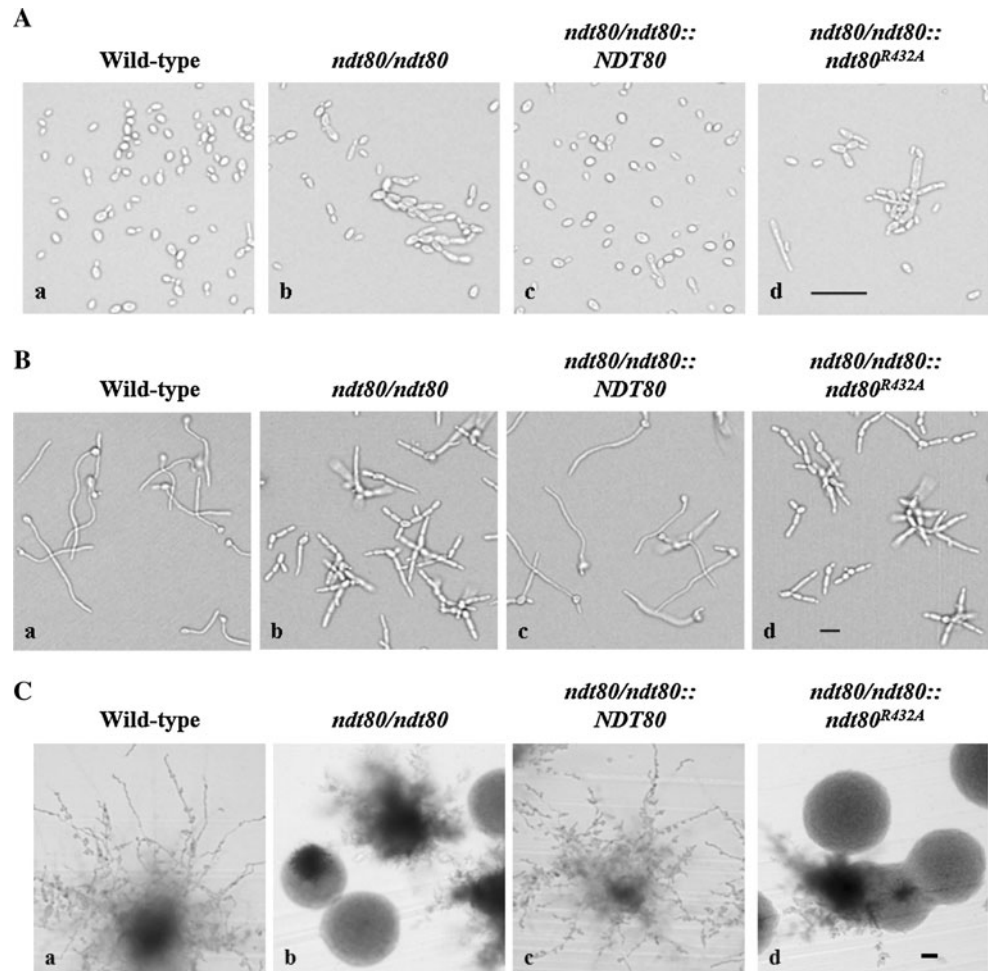
Fig. 3 Virulence assay in a mouse model. The BALB/c mice were injected with approximately 1×10^6 cells of the wild-type (SC5314, *filled squares*), *ndt80/ndt80* (YLO 386, *open squares*), *ndt80/ndt80::NDT80* (YLO464, *filled triangles*), or *ndt80/ndt80::ndt80* ^{R432A}-HA (YLO388, *open triangles*)

cells (Fig. 2Cb) were also defective in hyphal growth. A copy of the wild-type *NDT80* allele restored the ability to form germ-tube (Fig. 2Bc) and hyphae (Fig. 2Cc) of the *ndt80/ndt80* mutant cells. Our results demonstrate that Ndt80p is critical for cell separation, germ tube formation, and hyphal growth.

Mutations on *NDT80* diminish the virulence in a mouse model

We then investigated whether mutations on *NDT80* diminish the virulence in a mouse model of systemic infections. After 1 week, all mice injected with 1×10^6 wild-type cells died as expected (Fig. 3, solid squares). In contrast, all mice injected with the *ndt80/ndt80* mutant cells still survived (Fig. 3, open squares). A copy of the wild-type *NDT80* allele restored the virulence to the mutant cells (Fig. 3, solid triangles).

Ndt80p binds DNA with MSE

To investigate whether Ndt80p in *C. albicans* can bind DNA, we constructed strains expressing histidine-HA-tagged Ndt80p (Ndt80-HAp, Fig. 4A, lane 3) in the wild-type SC5314 background for immunoprecipitation against the HA tag. First, we conducted chromatin immunoprecipitation assays (CHIP) to enrich the chromatin DNA bound by Ndt80-HAp. We then performed PCR on the resulted DNA (Fig. 4B). The DNA fragments carrying the
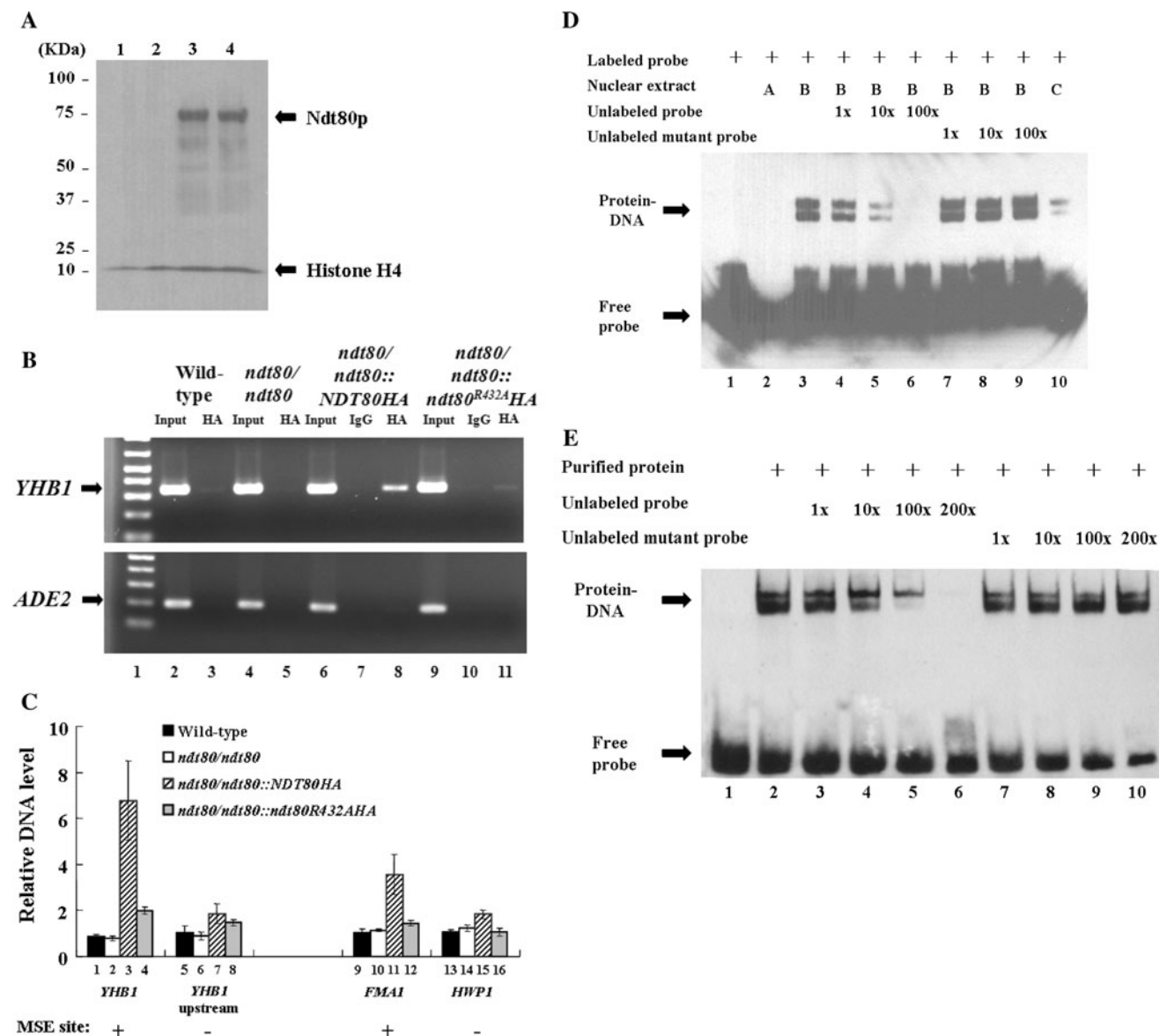
A

B

C

D

E

Fig. 4 DNA-binding assays. **A** The expression of HA-tagged protein of the wild-type (SC5314, *lane 1*), *ndt80/ndt80* (YLO386, *lane 2*), *ndt80/ndt80::NDT80-HA* (YLO387, *lane 3*), and *ndt80/ndt80:: ndt80^{R432A}-HA* (YLO388, *lane 4*) was determined by Western-blot analyses. The *lower bands* represent the loading control histone H4. **B** DNA fragments of the *YHB1* and *ADE2* promoters from different strains after CHIP were amplified by PCR. *Lanes 2*, *4*, *6*, and *9*, input genomic DNA alone; *lanes 3*, *5*, *8*, and *11*, CHIP in the presence of HA antibody; and *lanes 7* and *10*, CHIP in the presence of IgG non-specific antibody. **C** DNA fragments of various promoters from different strains after CHIP were amplified by real-time PCR. *YHB1* (*lanes 1–4*), *YHB1* upstream: 1.6–1.9 kbp upstream of *YHB1* (*lanes 5–8*),

FMA1 (*lanes 9–12*), and *HWP1* (*lanes 13–16*). **D** Ndt80p interacting with MSE. The labeled probes were incubated in the absence (*lane 1*) or presence of nuclear extracts from *ndt80/ndt80* (**A** YLO386, *lane 2*), *ndt80/ndt80::NDT80-HA* (**B** YLO387, *lanes 3* to *9*), and *ndt80/ ndt80::ndt80^{R432A}-HA* (**C** YLO388, *lane 10*) in the absence of unlabeled probe (*lanes 1–3* and *10*), presence of unlabeled probes (*lanes 4–6*), or unlabeled mutant probes (*lanes 7–9*). **E** Direct interaction between recombinant Ndt80p from *E. coli* and the MSE sequences. The labeled probes were incubated in the absence (*lane 1*) or presence (*lanes 2–10*) of recombinant Ndt80p from *E. coli*, in the absence of unlabeled probes (*lanes 1–2*), presence of unlabeled probes (*lanes 3–6*), or unlabeled mutant probes (*lanes 7–10*)

YHB1 promoters were amplified (Fig. 4B, upper panel, lane 8). In contrast, those carrying the *ADE2* promoters without MSE were not detected (Fig. 4B, bottom panel, lane 8).

To further determine the binding efficiency of Ndt80p to MSE, we performed real-time PCR on the resulted DNA

from the CHIP experiment to quantify DNA fragments carrying the promoters of various genes (Fig. 4C). As expected, the DNA of the *YHB1* promoter was enriched significantly by Ndt80-HAp (Fig. 4C, bar 2 vs. bar 3). The data also showed that the binding of Ndt80p to the *YHB1* promoter was sequence-specific since the DNA fragment

localized approximately 1.6–1.9 kbp upstream of *YHB1* was not enriched by Ndt80-HAp (Fig. 4C, bar 6 vs. bar 7). Furthermore, Ndt80-HAp also enriched other promoters with MSE, such as *FMA1*, a potential Ndt80p target gene identified by the DNA microarray analysis (Fig. 4C, bar 10 vs. bar 11), but not those without, such as *HWP1* (Fig. 4C, bar 14 vs. bar 15).

The electrophoretic mobility shift assays (EMSA) further supported the notion that MSE was the binding site of Ndt80p. When the labeled oligonucleotides containing MSE sequences were added to the nuclear extract from *ndt80/ndt80::NDT80-HA*, additional bands were present (Fig. 4D, indicated by the arrow marked protein-DNA). As the amount of the wild-type unlabeled probes increased, the intensity of the bands faded (Fig. 4D, lane 3 vs. lanes 4-6). In contrast, when the unlabeled mutant probe, with a base substitution in MSE, was used to compete with the wild-type labeled probes, the effect on the band intensity could be neglected (Fig. 4D, lane 3 vs. lanes 7-9). Hence, the interaction between Ndt80p and MSE could be titrated out by excessive amount of the unlabeled wild-type probes but not by the mutant ones. To assess whether Ndt80p directly binds MSE instead of being mediated by additional factors in the nuclear extract, we then performed EMSA with recombinant Ndt80p purified from *E. coli*. Our results showed that purified recombinant Ndt80p from *E. coli* could bind MSE directly (Fig. 4E, lane 2). Again, the interaction between Ndt80p and MSE could be titrated out by excessive amount of the unlabeled wild-type probes (Fig. 4E, lane 2 vs. lanes 5–6) but not by the mutated probes (Fig. 4E, lane 2 vs. lanes 9–10).

The R432 residue is important for all functions of Ndt80p

The residues responsible for DNA-binding capability of Ndt80p in *S. cerevisiae* have been reported. Among them, the R177 residue is the most important one. When this R177

residue is mutated, the DNA-binding capability decreases 27-fold in *S. cerevisiae* [25]. In a sequence comparison, the R432 residue in *C. albicans* corresponds to the R177 residue in *S. cerevisiae*. We recently found that the *ndt80^R432A* allele, containing a mutation on the DNA-binding domain, failed to complement the drug-sensitive phenotype caused by null mutations on *NDT80* in *C. albicans* [19]. Therefore, in the present study, we investigated whether R432A substitution also affected other functions of Ndt80p. The *ndt80^R432A* allele, unlike the wild-type, failed to restore to the *ndt80/ndt80* mutant cells the *YHB1* expression (Fig. 1A, bar 3 vs. bar 5), NaNO$_2$ sensitivity (Fig. 1B, *ndt80/ndt80::ndt80^R432A*), cell separation (Fig. 2Ad), germ tube formation (Fig. 2Bd), hyphal growth (Fig. 2Cd), and virulence in a mouse model (Fig. 3, open triangles).

According to the reported crystal structure of the Ndt80p DNA-binding domain of *S. cerevisiae*, we modeled the three-dimensional structure of Ndt80p DNA-binding domain of *C. albicans* using Phyre 2. The core structure of both proteins forms a β-sandwich with two antiparallel β sheets that consist of a three-stranded sheet and a four-stranded sheet. The strands in these two sheets are approximately perpendicular to the direction of those found in the β-sandwich. Besides that, the other structure comprises a continuous polypeptide chain with two short α-helices, helical turns, and also loop regions. Most importantly, like the R117 residue in Ndt80p DNA-binding domain of *S. cerevisiae*, the R432 in *C. albicans* is predicted to interact with DNA directly (Fig. 5). Additionally, the R432A substitution reduced the binding efficiency to MSE (Fig. 4D, lane 3 vs. lane 10), consistent with the CHIP result (Fig. 4B, C).

Discussion

Candida albicans may cause invasive infections when there are major dysfunctions in the host's cellular defense

Fig. 5 Predicated three-dimensional structures of Ndt80p DNA-binding domains. **A** Crystal structure of the Ndt80p DNA-binding domain in *S. cerevisiae* (PDB ID: 1mnn). **B** Predicted structure of the Ndt80p DNA-binding domain in *C. albicans* based on the structure of the homologue of *S. cerevisiae*. The R432 residue of *C. albicans* and its corresponding residue in *S. cerevisiae* are indicated by *arrows*
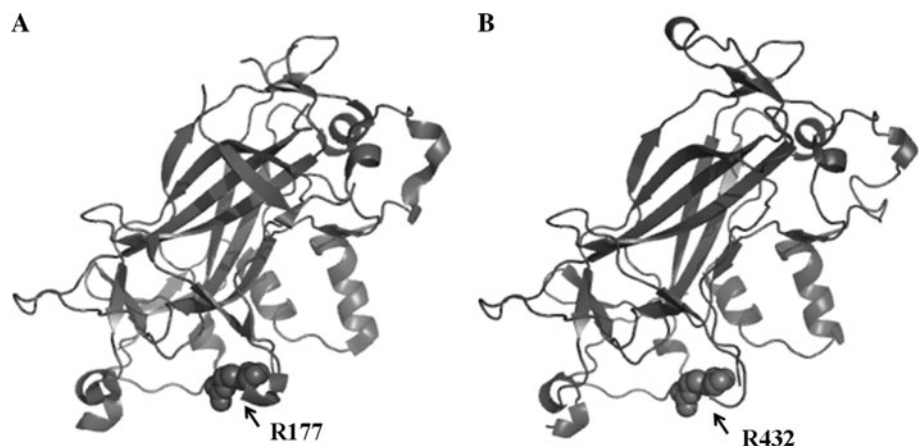
mechanisms. The two most well-defined mechanisms by which *C. albicans* can breach innate host defenses are the production of NO scavengers and the ability to penetrate macrophages by formation of hyphae. In the present study, we found that the DNA-binding domain of Ndt80p binds directly to MSE to regulate the expression of target genes involved in multiple signal transduction pathways in *C. albicans*. Most importantly, a single R432A substitution on the DNA-binding domain abolished all functions examined.

Initially, the *ndt80/ndt80* mutant cells generated from BWP17 were used for microarray and NO sensitivity assay. Since we have to construct new strains for the experiments in the present study, we chose SC5314 as the parental strain since the *SAT1* flipper cassette became available. Using the newly constructed strains, we found that Ndt80p bound to various promoters with diverse biological functions, consistent with the previous report [26]. Hence, *C. albicans* Ndt80p is an upstream modulator of the gene networks that respond to a variety of environmental conditions. To cope with stress such as exposures to antifungal drugs and NO, Ndt80p regulates different sets of genes, such as *CDR1*, *ERGs* [17, 26], and *YHB1*. It is interesting to determine whether Ndt80p regulates the basal and/or induced expressions of various targets.

Sellam et al. [20, 26] has reported a set of genes positively regulated by Ndt80p. Some, such as *YHB1* and *CHT3*, were also identified in the present study while others were not. Notably Sellam et al. did not find differences in the cell wall gene *HWP1*, which is the most highly down-regulated gene in the present study. We believe that the differences in the listed genes are due to different growth conditions. Cells were grown in YPD at 30°C by Sellam et al., but in YP containing 4% glucose pH 6.0 with 10 mM NaNO$_2$ at 37°C in the present study. Furthermore, cells were grown in the presence of NaNO$_2$ instead of azole drugs. Subsequently, *CDR1* was not identified in the present study.

The eukaryotic nature of fungi reduces the number of potential antifungal targets. Hence, the limited choices of clinically active antifungal drugs and the emerging drug resistance are major issues in managing fungal infections. Our findings further support that the Ndt80p of *C. albicans* recognizes MSE just as Ndt80p of *S. cerevisiae* does [26]. Furthermore, the R432A substitution in the Ndt80p DNA-binding domain blocks its functions in cell separation, drug resistance, NO inactivation, germ tube formation, hyphal growth, and virulence in *C. albicans*, suggesting a novel target for new antifungal drugs.

References

1. Tusher VG, Tibshirani R, Chu G (2001) Significance analysis of microarrays applied to the ionizing radiation response. Proc Natl Acad Sci USA 98:5116–5121
2. Cheng MF, Yu KW, Tang RB, Fan YH, Yang YL, Hsieh KS, Ho M, Lo HJ (2004) Distribution and antifungal susceptibility of *Candida* species causing candidemia from 1996 to 1999. Diagn Microbiol Infect Dis 48:33–37
3. Pappas PG, Rex JH, Lee J, Hamill RJ, Larsen RA, Powderly W, Kauffman CA, Hyslop N, Mangino JE, Chapman S, Horowitz HW, Edwards JE, Dismukes WE (2003) A prospective observational study of candidemia: epidemiology, therapy, and influences on mortality in hospitalized adult and pediatric patients. Clin Infect Dis 37:634–643
4. Yang YL, Ho YA, Cheng HH, Ho M, Lo HJ (2004) Susceptibilities of *Candida* species to amphotericin B and fluconazole: the emergence of fluconazole resistance in *Candida tropicalis*. Infect Control Hosp Epidemiol 25:60–64
5. Yang YL, Li SY, Cheng HH, Lo HJ (2005) Susceptibilities to amphotericin B and fluconazole of *Candida* species in TSARY 2002. Diagn Microbiol Infect Dis 51:179–183
6. Blasi E, Pitzurra L, Puliti M, Chimienti AR, Mazzolla R, Barluzzi R, Bistoni F (1995) Differential susceptibility of yeast and hyphal forms of *Candida albicans* to macrophage-derived nitrogen-containing compounds. Infect Immun 63:1806–1809
7. MacMicking J, Xie QW, Nathan C (1997) Nitric oxide and macrophage function. Annu Rev Immunol 15:323–350
8. Rementeria A, Garcia-Tobalina R, Sevilla MJ (1995) Nitric oxide-dependent killing of *Candida albicans* by murine peritoneal cells during an experimental infection. FEMS Immunol Med Microbiol 11:157–162
9. Hromatka BS, Noble SM, Johnson AD (2005) Transcriptional response of *Candida albicans* to nitric oxide and the role of the *YHB1* gene in nitrosative stress and virulence. Mol Biol Cell 16:4814–4826
10. Ullmann BD, Myers H, Chiranand W, Lazzell AL, Zhao Q, Vega LA, Lopez-Ribot JL, Gardner PR, Gustin MC (2004) Inducible defense mechanism against nitric oxide in *Candida albicans*. Eukaryot Cell 3:715–723
11. Chiranand W, McLeod I, Zhou H, Lynn JJ, Vega LA, Myers H, Yates JR 3rd, Lorenz MC, Gustin MC (2008) *CTA4* transcription factor mediates induction of nitrosative stress response in *Candida albicans*. Eukaryot Cell 7:268–278
12. Chen CG, Yang YL, Cheng HH, Su CL, Huang SF, Chen CT, Liu YT, Su IJ, Lo HJ (2006) Non-lethal *Candida albicans cph1/cph1 efg1/efg1* transcription factor mutant establishing restricted zone of infection in a mouse model of systemic infection. Int J Immunopathol Pharmacol 19:561–565
13. Lo HJ, Kohler JR, DiDomenico B, Loebenberg D, Cacciapuoti A, Fink GR (1997) Nonfilamentous *C. albicans* mutants are avirulent. Cell 90:939–949

14. Murad AM, d'Enfert C, Gaillardin C, Tournu H, Tekaia F, Talibi D, Marechal D, Marchais V, Cottin J, Brown AJ (2001) Transcript profiling in *Candida albicans* reveals new cellular functions for the transcriptional repressors *CaTup1*, *CaMig1* and *CaNrg1*. Mol Microbiol 42:981–993

15. Murad AM, Leng P, Straffon M, Wishart J, Macaskill S, Mac-Callum D, Schnell N, Talibi D, Marechal D, Tekaia F, d'Enfert C, Gaillardin C, Odds FC, Brown AJ (2001) *NRG1* represses yeast-hypha morphogenesis and hypha-specific gene expression in *Candida albicans*. EMBO J 20:4742–4752

16. Braun BR, Johnson AD (1997) Control of filament formation in *Candida albicans* by the transcriptional repressor *TUP1*. Science 277:105–109

17. Chen CG, Yang YL, Shih HI, Su CL, Lo HJ (2004) CaNdt80 is involved in drug resistance in *Candida albicans* by regulating *CDR1*. Antimicrob Agents Chemother 48:4505–4512

18. Chu S, Herskowitz I (1998) Gametogenesis in yeast is regulated by a transcriptional cascade dependent on Ndt80. Mol Cell 1:685–696

19. Wang JS, Yang YL, Wu CG, Ouyang KJ, Tseng KY, Chen CG, Wang H, Lo HJ (2006) The DNA binding domain of CaNdt80p is required to activate *CDR1* involved in drug resistance in *Candida albicans*. J Med Microbiol 55:1403–1411

20. Sellam A, Askew C, Epp E, Tebbji F, Mullick A, Whiteway M, Nantel A (2010) Role of transcription factor CaNdt80p in cell separation, hyphal growth, and virulence in *Candida albicans*. Eukaryot Cell 9:634–644

21. Sherman F (2002) Getting started with yeast. Methods Enzymol 350:3–41

22. Sohn K, Senyurek I, Fertey J, Konigsdorfer A, Joffroy C, Hauser N, Zelt G, Brunner H, Rupp S (2006) An in vitro assay to study the transcriptional response during adherence of *Candida albicans* to different human epithelia. FEMS Yeast Res 6:1085–1093

23. Reuss O, Vik A, Kolter R, Morschhauser J (2004) The *SAT1* flipper, an optimized tool for gene disruption in *Candida albicans*. Gene 341:119–127

24. Guthrie C, Fink GR (2002) Guide to yeast genetics and molecular biology, part C. Methods Enzymol 351:190–192

25. Montano SP, Cote ML, Fingerman I, Pierce M, Vershon AK, Georgiadis MM (2002) Crystal structure of the DNA-binding domain from Ndt80, a transcriptional activator required for meiosis in yeast. Proc Natl Acad Sci USA 99:14041–14046

26. Sellam A, Tebbji F, Nantel A (2009) Role of Ndt80p in sterol metabolism regulation and azole resistance in *Candida albicans*. Eukaryot Cell 8:1174–1183

27. Gillum AM, Tsay EY, Kirsch DR (1984) Isolation of the *Candida albicans* gene for orotidine-5′-phosphate decarboxylase by complementation of *S. cerevisiae ura3* and *E. coli pyrF* mutations. Mol Gen Genet 198:179–182